The Heat Transfer Modeling for Minimization of Thermal Necrosis in Hip Resurfacing Arthroplasty

BEE 4530

Daniel Baskind, Hyunjin Kim, Flora Min, Hyeongsu Park

April 30, 2009

Table of Contents

1. Executive Summary

In the past, the only option for replacing broken or otherwise malfunctioning hip bones was total hip replacement (THR), which involved the removal of the body's natural hip joint and replacing it with an entirely synthetic joint. However, the complications involved with such extensive surgery have led to the push for less invasive therapies. One such idea that has gained popularity for younger patients is hip resurfacing arthroplasty (HRA), which focuses on repairing the joint rather than entirely replacing it. However, there are some issues with HRA, namely thermal bone necrosis due to the heat of polymerization during cement hardening.

This paper examines this necrosis as well as the thermal trends of hip resurfacing surgery through the use of COMSOL, a computer aided engineering tool. In COMSOL, a 2D-axisymetric geometry was developed to model the leg bone, cement, ball, cap, and the hipbone. Boundary condition and initial condition was set to portray a realistic surgical environment. With the objective of minimizing bone necrosis, the model's parameters were adjusted to simulate a variety of material properties (different prosthetic material, and different bone conditions), as well as plausible surgical conditions (pre-cooled cement, and convective cooling). Sensitivity analysis was also conducted to gain a better understanding of the thermal tendencies of HRA. Based on the data from these simulations we were able to provide some insight into what approaches may be best for minimizing the extent of the thermal necrosis. The following paragraphs describe the most significant among these conclusions.

First of all, we found that precooling the implant from room temperature to 5°C resulted in a drop in the maximum temperature by 7°C. It appears that precooling the cement in addition to the implant had no additional significant temperature reduction. Also, our sensitivity analysis revealed that our system was most sensitive to changes in precooling temperature. All of these factors seem to suggest that precooling may be an effective means for reducing thermal bone necrosis.

Secondly, simulations of cancellous bone showed a maximum temperature lower than that of normal bone. As cancellous bone is typical of elderly patients, these results suggest that there is a lower risk of complications due to thermal necrosis during HRA for elderly patients than for younger individuals.

Third, when varying our parameters, we often incurred computational failure due to the presence of "hot spots," small regions of the cement that reached extremely high values. Our sensitivity analysis revealed that our system at its default parameter values was extremely close to values that resulted in these hot spots. While it's questionable if these hot spot events are consistent with realistic physics, the topic deserves further investigation considered the potentially damaging results.

While our model does not conclusively provide guidelines for reducing thermal necrosis, it does provide some ideas for successful prevention. Computational analysis as a first step helps us understand the thermal effects of HRA and sets the stage for subsequent experimentation.

2. Introduction

Arthroplasty is the replacement or repair of damaged bones through surgical means with metals or ceramics. Currently, hip arthroplasty is divided into two major approaches: total hip replacement (THR) and a more recent development, hip resurfacing arthroplasty (HRA). HRA focuses on repairing the hip joint (rather than entirely replacing it as in THR), allowing for a minimally invasive surgical procedure. While HRA has proved to be less intrusive than THR, one major complication is thermal necrosis caused by the polymerization of the cement mantle that takes place during surgery.

HRA has gained popularity among younger patients, but isn't seen as an option for elderly patients. Cancellous bone, typically found in elderly patients, is weaker than normal bone, and is highly susceptible to breakage, especially after surgery. The risk of additional bone weakness due to thermal necrosis has made surgeons hesitant to use HRA on older patients. Instead, surgeons prefer to entirely replace the load-bearing components of the hip joint rather than deal with the risks associated with attempting to repair them.

The cement mantle is responsible for adhesion between the implant parts and the bone. A popular choice is polymethyl methacrylate (PMMA), often used due to its cheap price and short solidification time. However, heat generated from polymerization has been shown to cause thermal osteo-necrosis around the hip replacement, and several papers reported that the bone temperature surrounding the hip replacement can go as high as 55˚C to 60˚C (Li, 2003 & Chandler, 2005). Furthermore, heat dissipation from the hip socket to the surrounding tissue might cause vascular, nerve, and visceral damage near the pelvis. One clinical case showed that urological complications can occur due to excess heat generation from the hip replacement as the bladder and the ureter are in close proximity to the replacement (Videbaek, 1985 & Greenspan, 1978).

A. Design Objectives

The goal of this project is to model the heat transfer pattern of a hip joint system with resurfacing arthroplasty. Our design objectives in this project are three-fold: 1) establish a quantified measurement of thermal necrosis in terms of exposure time and temperature; 2) determine the heat generation equation from polymerization kinetics model of PMMA; and 3) organize an appropriate objective function to minimize thermal bone necrosis and the maximize the degree of polymerization of the cement at the end of surgery (the cement must be fully polymerized for sufficient adhesion).

Through this objective function, we will be able to quantitatively evaluate the merits of a variety of surgical options. First of all, we will simulate a variety of materials for the implant. Secondly, we will test different precooling conditions for both the implant parts and the cement. By developing a realistic and quantitative model of the thermal conditions of HRA, we hope to optimize these parameters to gain insight into potential improvements for this surgery.

Furthermore, despite several significant advantages offered by HRA over THR, the potential complications of HRA in elderly patients has prevented the technique from becoming widely accepted in the orthopedic surgical community. Nonetheless, the minimally invasive procedure afforded by HRA could be particularly advantageous in elderly patients, given the faster and easier recovery. Thus, we will also consider the thermal effects of HRA on cancellous bone, typically found in older patients.

B. Schematic

Initially, our project was based on the full 3-D geometry of a human femur. After borrowing an accurate femur replica, we were able to construct a computer-aided design (CAD) model using a 3-D laser scanner. However, the scanner was only able to provide detailed scanning along certain geometric planes, which resulted in a broken geometry that wasn't compatible with COMSOL (**Figure 1**, left). We then attempted to repair the geometry using Materialise Magics, a program capable of manipulating CAD meshes. Through the use of a number of the Magics modules, we were able to obtain a more complete geometry (**Figure 1**, right).

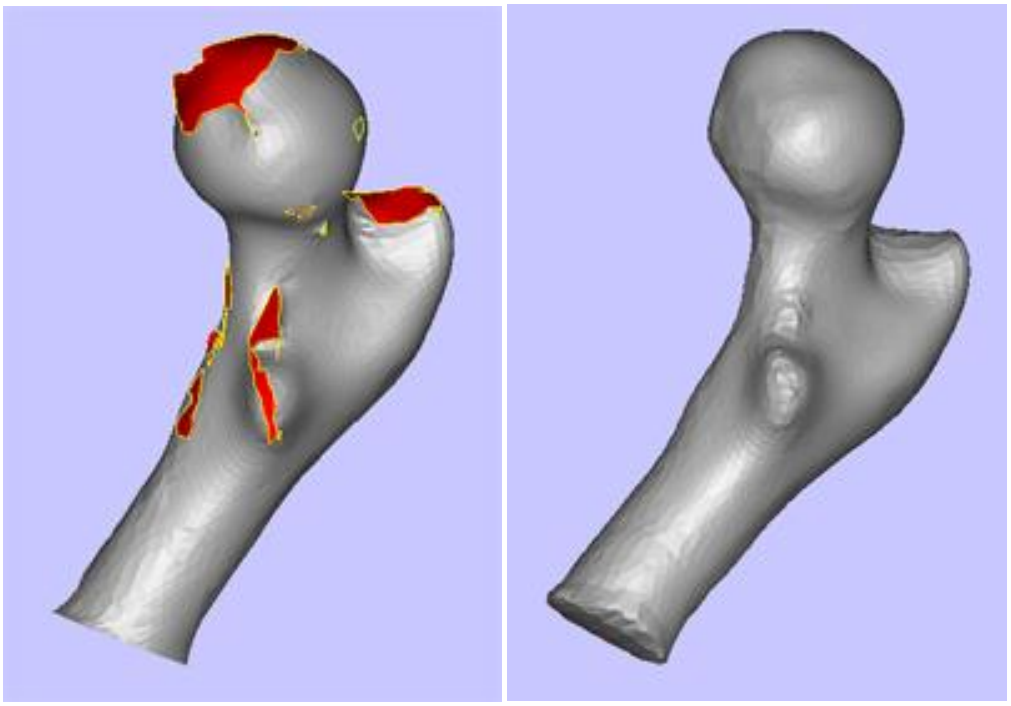

Figure1. Repairing the CAD geometry. After using a 3-D laser scanner, the CAD model was repaired using MaterialiseMagics.

While the resulting CAD model was COMSOL compatible, we struggled with adding the other components of the implant (i.e. setting up a boundary for the bone cement). Thus we were forced to abandon our scanned geometry and construct a 2-D model from scratch. However, this alternative approach was not necessarily at an expense of accuracy. It is true that the 3-D model better accounted for the bone's geometry, however our current 2-D axisymmetric model is closer to the "perfect" spherical geometry of real hip joint prosthesis. The rest of this report focuses on those efforts.

The constructed 2-D axisymmetric model is shown in **Figure 2** with the dimensions there shown. Moving outward from the center, the metal ball element is driven into the biologically-active femur bone. Then there is the adhesive cement, the surfacing part of the ball, the cap, another layer of cement, then the hip bone. We model these 7 layers with 3 different sets of

material properties (metal, cement, bone). The dotted yellow line shown in **Figure 2** corresponds to a convective boundary condition, simulating a fan during surgery.

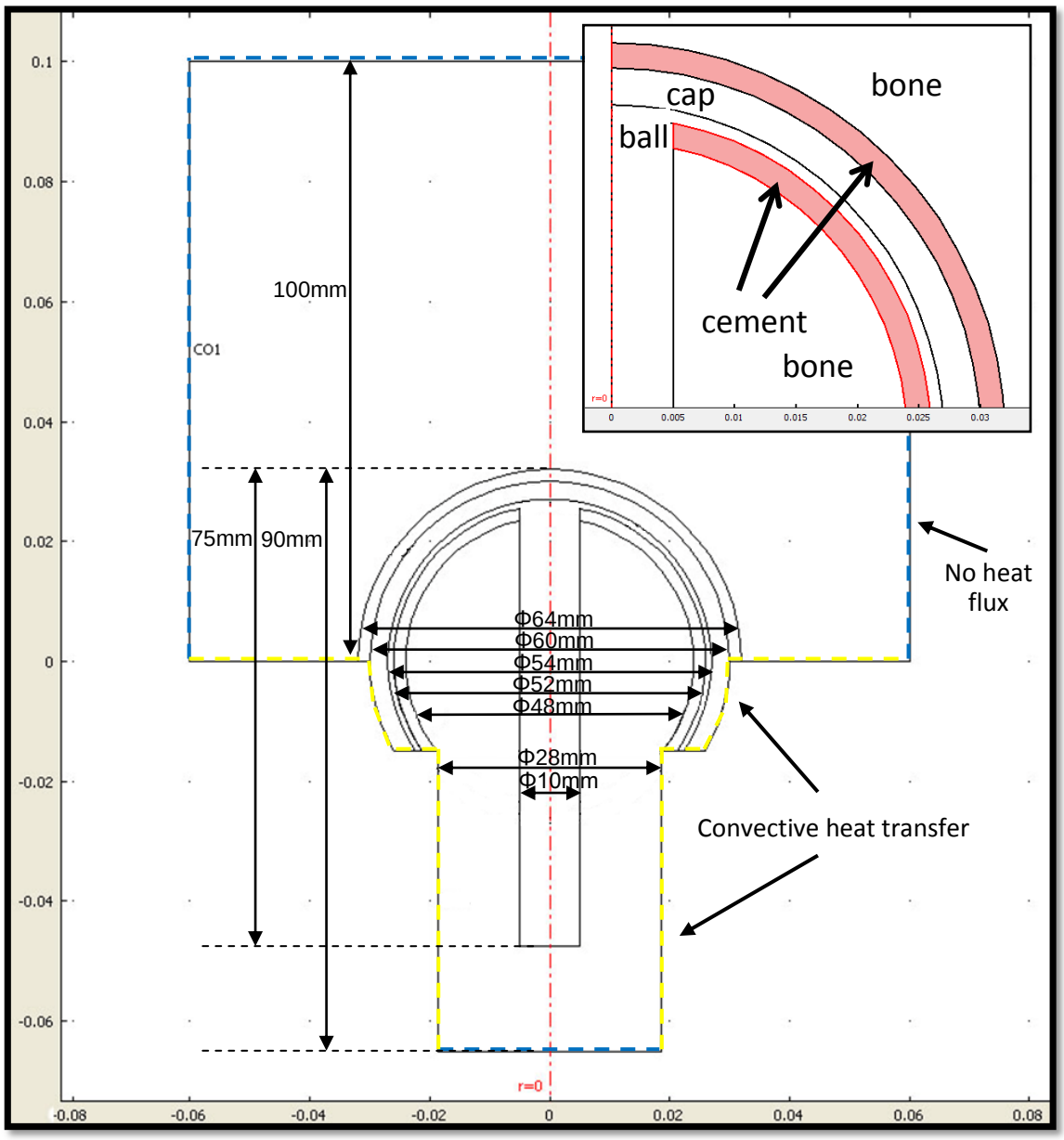

Figure 2. Schematic of the hip replacement system (axi-symmetric with respect to the red center vertical line)

C. Mathematics

The mathematics for our system involved the heat transfer equation with transient, conductive, and source terms. The source term generated heat depending on the degree of polymerization of the cement. We were able to calculate the volumetric heat generation through a differential equation in terms of the degree of polymerization. Thermal necrosis was also modeled through the use of a differential equation. Both of these systems were implemented in

COMSOL using a species solver. The details for these procedures as well as the other mathematical specifics (i.e. boundary and initial conditions) can be found in Appendix A.

D. Material Properties

In order to simulate the use of different materials for the implant, we obtained values for thermal conductivity, density, and specific heat capacity from the literature. The materials we are considering are Cobalt-Chromium alloy (CoCr), Zirconium, Tantalum, and Alumina. These parameter values can be found in Appendix A. During the procedure for simulating different bone conditions, we were able to obtain values for thermal conductivity, density, and specific heat capacity from the literature for both normal bone and cancellous bone. We did not vary the properties of bone cement, as PMMA seems to be the indisputable choice. PMMA is provided as a white powder and is mixed with a monomer fluid of MMA(Methyl Methacrylate) at the operation table with a catalyst that starts the polymerization of the fluid portion (our heat source term of interest for this project).

In our simulation of the convective boundary condition, we assumed that air is at room temperature, which is the case in a typical surgery room for which Throne (1996, p.124) suggested a heat transfer coefficient value of 10-100 W/m^2K. We ended up using 100 W/m^2K given that it corresponds to a blower with air velocity of 10m/s from our calculation of the convective heat transfer coefficient.

In our discussion of our results below, only the parameter or set of parameters being discussed is changed. Otherwise, they are kept at their default values. These values along with the other testing values are displayed in **Table 1** in Appendix A.

3. Results and Discussion

Unfortunately, some computational problems prevented us from using thermal necrosis factor Ω to measure the degree of thermal necrosis. Instead, we used the maximum temperature reached by a representative point in the bone tissue.

Although the direct cause was indeterminable, we found that Ω was not working properly. This is illustrated in **Figure 3**. In this solution, the Ω profile in femur and pelvic bones showed that the maximum Ω value was 0.0765. This value is much lower than the threshold value for necrosis of 0.4, which would seem to indicate that there is no thermal necrosis at all. However, since the temperature of the bone went as high as 60C, we should be seeing values greater than Ω = 0.4. Such high temperature is clearly seen in the temperature contour plot, while the contour plot of the thermal necrosis factor indicated differently.

Thus the problem regarding the thermal necrosis factor was recognized, and we decided to define the degree of thermal necrosis by the temperature. Since we know that any temperature above 43C is prone to thermal necrosis, the maximum temperature of the bone was examined for all of our results.

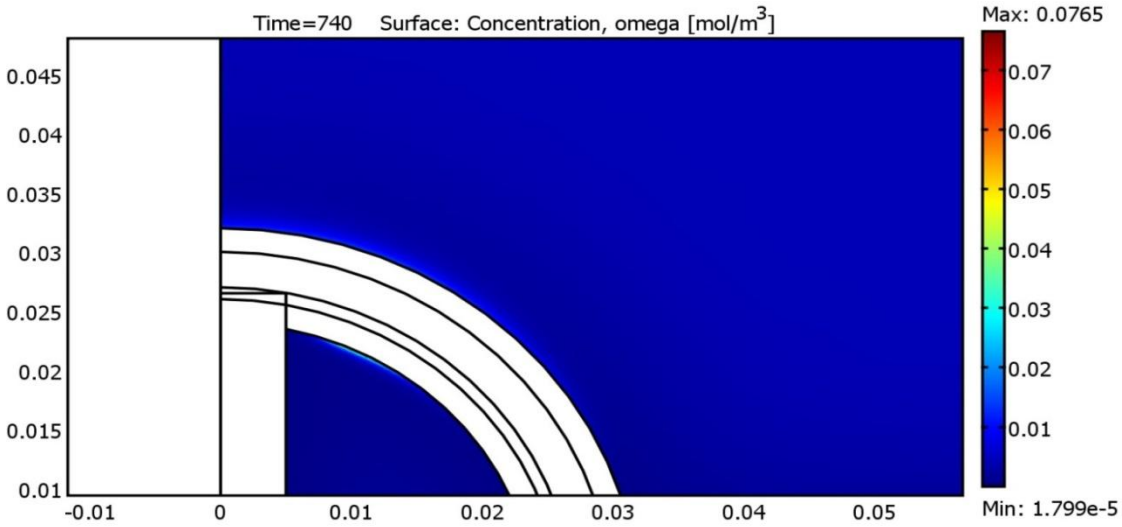

Figure 3.Omega concentration profile in femur and pelvic bones. The Maximum only reached to 0.0765, far less value than the expected values from the analysis of the temperature contour plot solution.

A. The Typical Solution

The following is a description of the solution using the default values (**Table 1** in Appendix A, red columns). **Figure 4** gives a good representation of the temperature profile for any point in the cement coordinate [0.011823,0.022375]) and the bone adjacent to the cement. At first (500s – 600s), heat generation does not appear to start. The only heat transfer is diffusion from the body-temperature bone to the room-temperature cement and implant. Then, at around 700s, cement polymerization begins and proceeds to completion very rapidly (~50s).

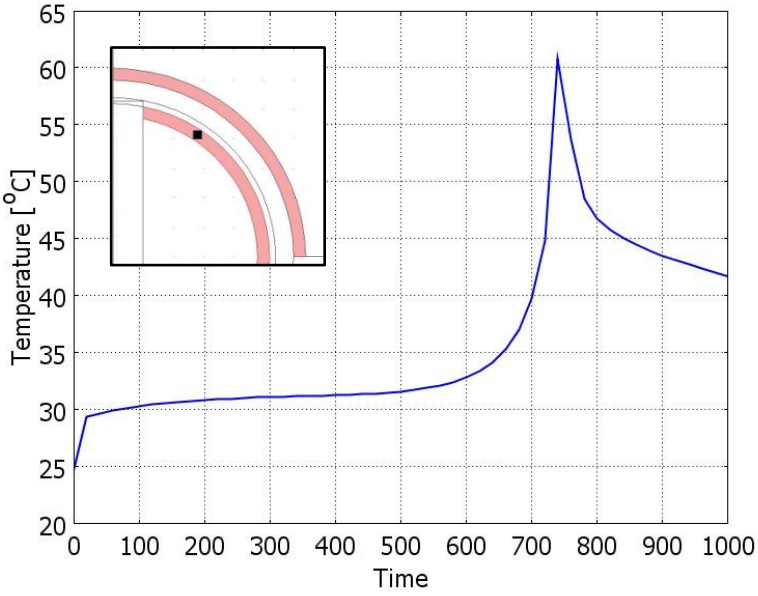

Figure 4. Temperature profile of the cement (at the point of the maximum temperature). The coordinate is indicated as ■. (coordinate [0.011823,0.022375])

Relative to the long preliminary stage without heat generation, the surge of polymerization and heating is quite rapid. This sudden reaction can be explained by the positive feedback loop between temperature and the degree of polymerization. As one can see in the differential equation for α, the degree of polymerization (Appendix A), the main driving force of polymerization is high temperature in Arrhenius term. When the temperature of the cement is increased by the heat diffusion from the surrounding tissues, the rate of polymerization is increased. This in turn generates more heat and increases the temperature, completing the loop between the temperature and the degree of polymerization.

Interestingly, the temperature increase does not happen in the entire cement region at the same time, instead propagating outward from the axis of symmetry toward the convective surface. This makes sense because air convection from the surface constantly decreases the temperature, and the region near the axis of symmetry is least subject to convective cooling. Also, the cap cement is adjacent to the larger surface area of warm tissue and should reach the temperature that triggers rapid polymerization before the ball cement on the inside would. Then, the heat generated from one point in the cement increases the temperature of the surrounding cement and triggers the temperature surge. This serial heat generation results in a domino effect, causing a wave-like propagation in temperature increase.

Although the inner and outer cement both undergo increases in temperature, the temperature of inner cement increases more rapidly and reaches a higher temperature than the outer cement. As seen in **Figure 5**, the inner cement temperature reaches 63˚C at 760s, whereas the outer cement is around 40˚C over the broad region. This observation can be accounted for by the same logic we used to explain the early temperature surge of the outer cement: once the outer cement temperature surpasses the tissue temperature, the heat diffuses out from the cement to the tissue, and the outer cement loses heat more rapidly than the inner cement because of its larger surface area. Thus, the rate of temperature growth is restricted by heat diffusion in the outer cement.

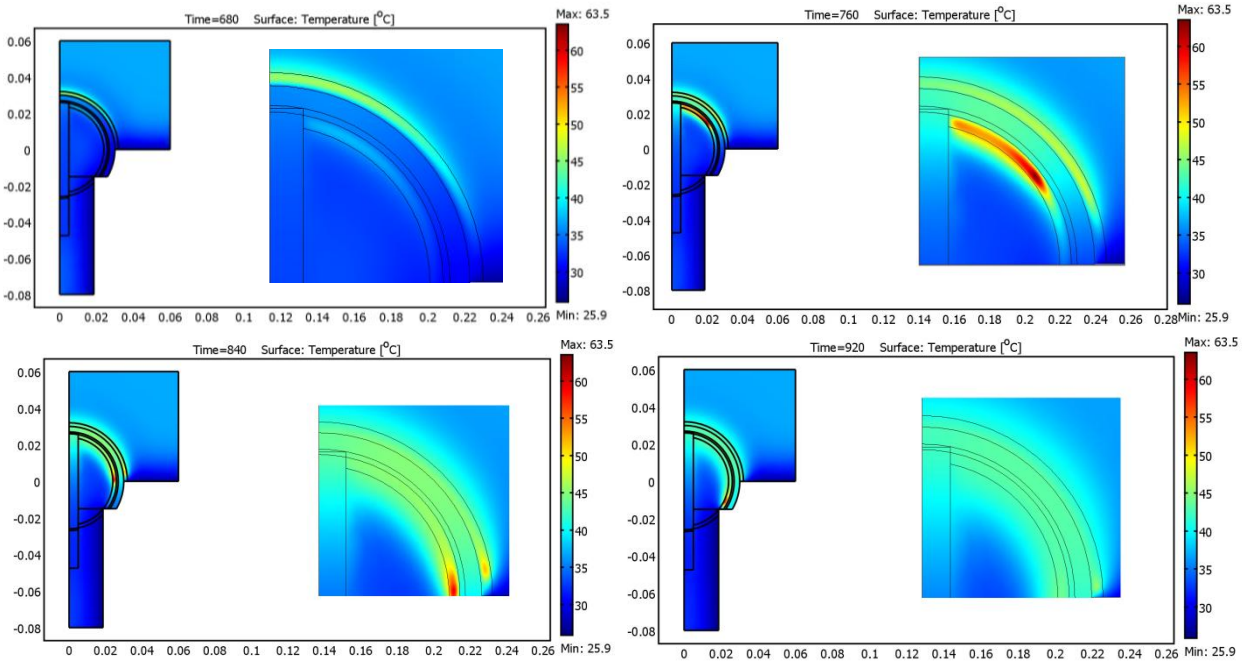

Figure 5. Temperature contour at the onset of polymerization

The increase in the degree of polymerization is coincident with the increase in temperature. The degree of polymerization gradually increases up to 0.2, and after that point, polymerization rapidly proceeds to 0.9 (90%) within 50s. Once it almost reaches 1, the derivative of the degree of polymerization with respect to time (slope in **Figure 6**) becomes flat and the volumetric heat generation also approaches to zero. In **Figure 7**, at 760s, the region near the symmetric axis has already gone through the complete polymerization while the rest of the cement has not begun to polymerize. The time of hot spot generation in the cement region corresponds to the initial time of the polymerization propagation. This can be seen by the comparison between the degree of polymerization in **Figure 8** and the temperature profile in **Figure 7.**

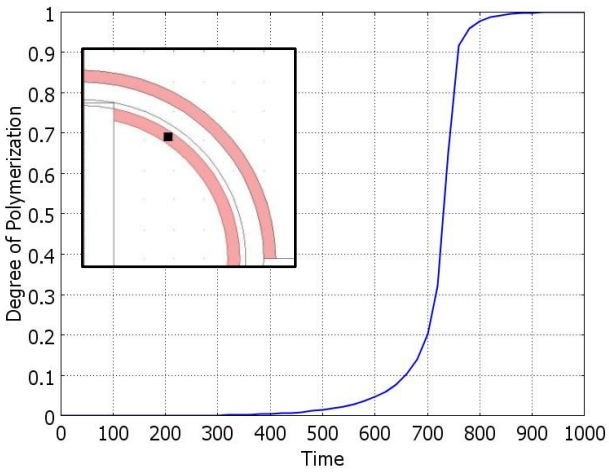

Figure 6. Profile of the degree of polymerization of the cement at the coordinate as indicated (■).(coordinate [0.011823,0.022375])

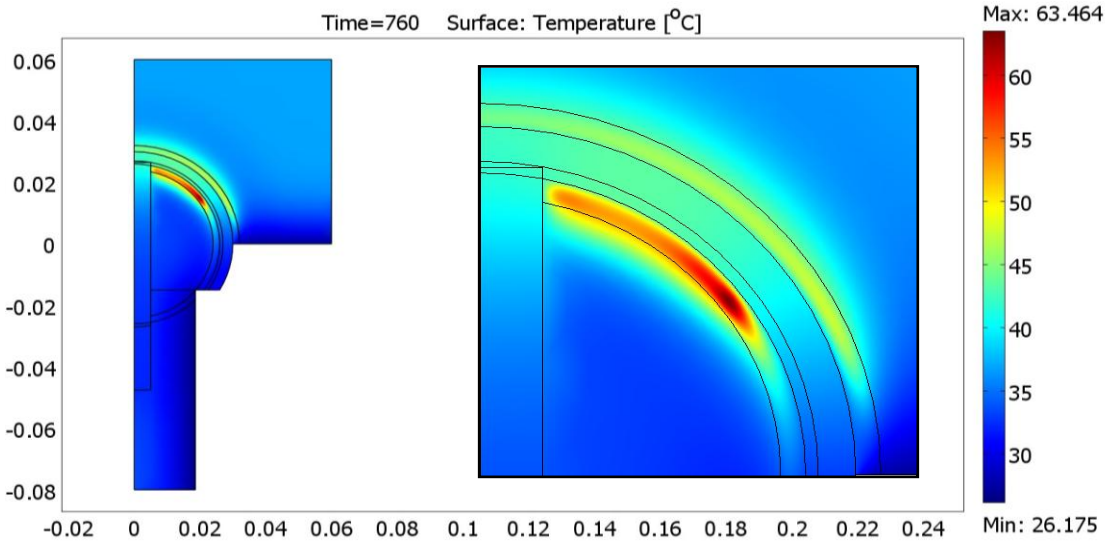

Figure 7. Temperature profile at 760 s (when the temperature reaches its maximum)

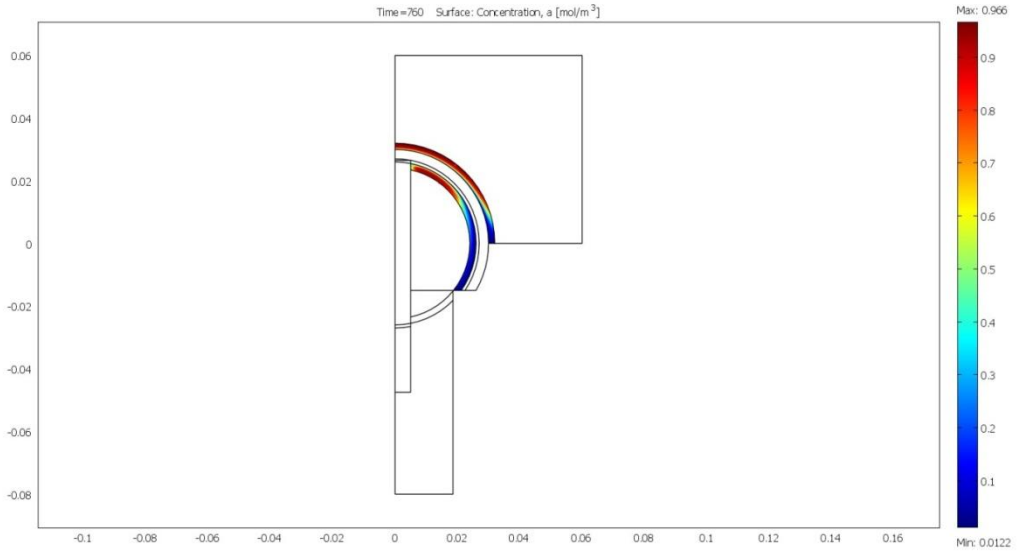

Figure 8. Degree of polymerization at 760 seconds. In order to model the source term, implemented the degree of polymerization using a COMSOL diffusion physics system.

B. Test Conditions

The temperature profile up to 2000 seconds at the two specified coordinates of the bone was taken after our system was run in COMSOL. The two coordinates were located (one in pelvic bone region and one in femur bone region) by finding where the temperature is highest after the system ran up to 2000 seconds. For our analysis, the coordinate in the femur region was taken (coordinate [0.010965,0.020086]) because the femur bone tissue was heated slightly more than the pelvic bone at all time steps. Since we are interested in the maximum temperatures that healthy bone tissue reaches, any T_{max} in the femur was taken to be the T_{max} that any surrounding bone tissue reaches. The degree of polymerization (ranging from 0 to 1) was also plotted at a specified coordinate (chosen near the center, coordinate [0.011823,0.022375]) inside the cement. In all cases, the polymerization was complete well before the 2000 seconds period.

Cancellous Bone

The default values and those for cancellous bone reached the maximum temperatures of 47.2˚C and 45.8˚C respectively, both around 760 seconds (**Figure 9**). Interestingly, this suggested that the patients with cancellous bone are less prone to getting thermal necrosis during the surgery, given that the surgical procedure was identical. After the temperature reached its peak, it cooled down to temperatures lower than 43˚C in both cases.

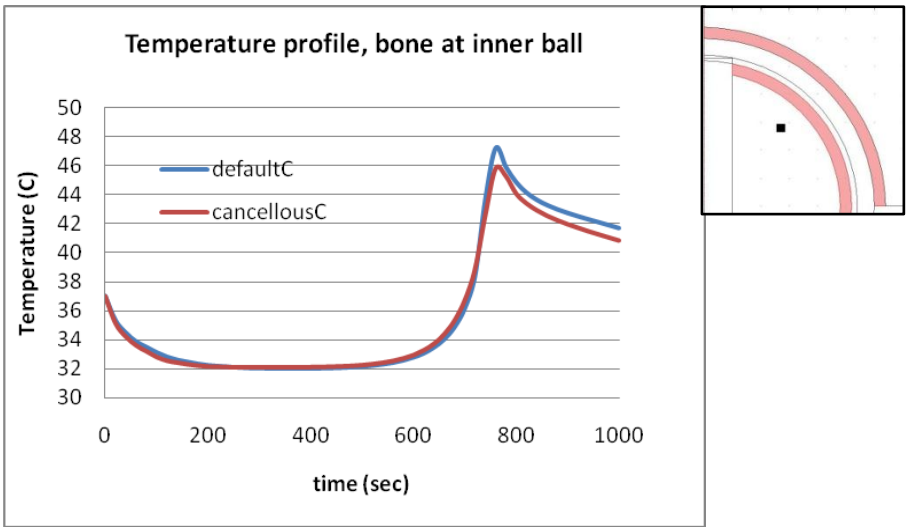

Figure 9. The temperature profile of the bone in the shown coordinate as indicated (■) within the femur bone region. (coordinate [0.010965,0.020086]) T_{max} is reached near 48˚C, for both the default values and the cancellous bone values.

Precooling

In order to test precooling, we considered two scenarios other than the default values: 1) cooling the cement and the implant and 2) cooling just the implant. For our purposes, cooling meant lowering the initial temperature to 5˚C. In both cases, the maximum temperature value decreased by about 7˚C, meaning there wasn't much of a difference between the two precooling conditions (**Figure 10**). This suggests that either scenario would provide the means to decrease thermal necrosis. However, we expect that precooling the cement may prolong the time it takes to polymerize. Thus, one could conclude that cooling just the implant and not the cement provides sufficient precooling for our purposes.

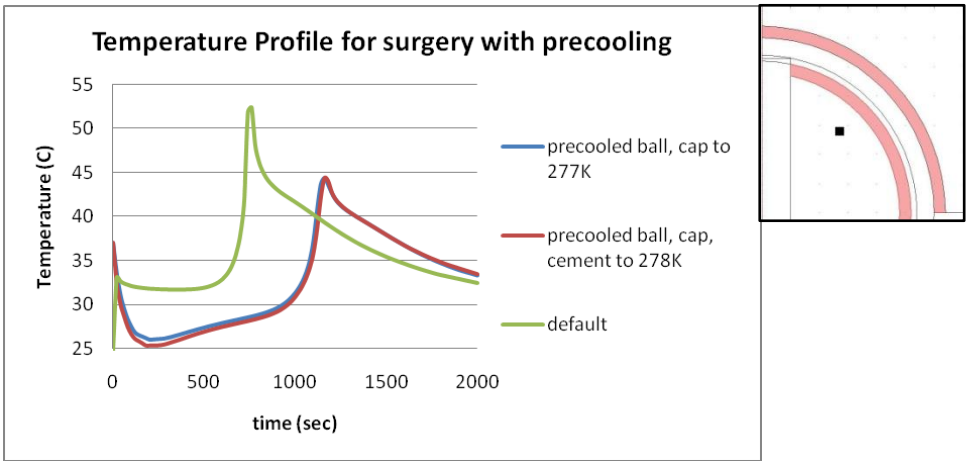

Figure 10.Temperature profile of surgery with and without precooling. The default (no precooling) curve and the two precooling curves differ greatly, although the two different precooling conditions differed minimally from each other. The coordinate where the temperature profile was drawn is indicated on the contour plot as ■. (coordinate [0.010965,0.020086])

C. Computational Failure

Unfortunately, we were not able to generate solutions for scenarios including different implant materials. This was due to computational failures of COMSOL near 700-1000 seconds, when the solver displayed an "infinity residual error" and stopped solving the heat equation. We analyzed the source of this computational error by plotting surface plots of all the variables, their derivatives, and terms in the governing equation.

Although we were not able to exactly define where the problem came from, it appears that it originates in the cement hotspot mentioned previously. In this case, we believe that the value of the volumetric heat generation term grows large enough to cause a computational error. On the surface plot, the shape of the hot spot looks similar to that in **Figure 7**. **Figure 11** describes the change of volumetric heat generation at the hot spot with time in a case where the solver could proceed until 2000s. Volumetric heat generation reaches up to $3.5 \cdot 10^6 W/m^2$ due to a rapid change in degree of polymerization. We believe that in the erroneous case, the previously mentioned the positive feedback loop may make the system computationally unstable during heat generation. In other words, during the solution process, COMSOL's function for evaluating error (i.e. comparing solutions between different time-step sizes) may result in a rapidly growing residual.

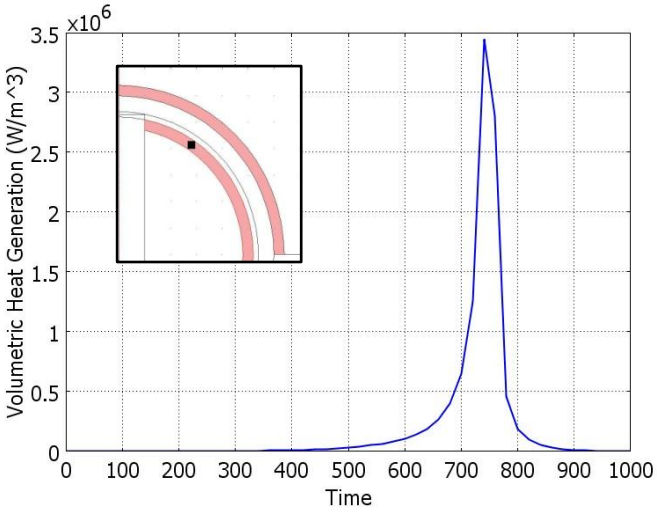

Figure 11. Volumetric heat generation Q (in W/m^3) at the coordinate as indicated (■). (coordinate [0.011823,0.022375]) In order to model the source term, we implemented the degree of polymerization using a COMSOL diffusion physics system.

D. Sensitivity Analysis

In order to better understand our system, we conducted a sensitivity analysis. The sensitivity analysis provides us 1) an understanding of how accurate we need to be with our chosen parameter values and 2) an understanding of how influential a particular test parameter is to our objective function (in this case T_{max}). We would have liked to also do an uncertainty analysis for our bone parameter values (red column, **Table 1** in Appendix A) as we found a variety of values in the literature for normal bone. This would give us an estimate of the error range in our solution, given this uncertainty.

In order to determine the sensitivity of the system to variation of parameters at its default values (found in Appendix A, **Table 1**), we tested for changes in the maximum bone temperature value at our test point. We changed the parameter by +5% and -5% of its default value and calculated the change in the maximum temperatures. However, due to solution errors, we were not able to obtain both values in each case. Even when reducing the sensitivity range to +0.5% and -0.5%, we were not able to generate a two-sided analysis. This suggests that our default values are very close to a nonconvergent state.

In terms of our material values (all values but the first two), this sensitivity seems acceptable. In **Figure 12**, the 5% sensitivities are below a 0.25°C change in T_{max}, which is certainly sufficient given the confidence we have in our metal values (high uniformity among metals, and well tested). While we are less confident in our bone values, the sensitivity there is even less. Though we would be able to analyze this more effectively with an uncertainty analysis, these sensitivity values make it seem that our solution is reasonably accurate.
We found that the sensitivities of ρ and C_p are the same. This makes sense considering the governing equation being considered (Appendix A). These values are included as a product in that equation, thus a 5% change in either parameter would yield the same product. In other words, the two sensitivity tests are mathematically identical.

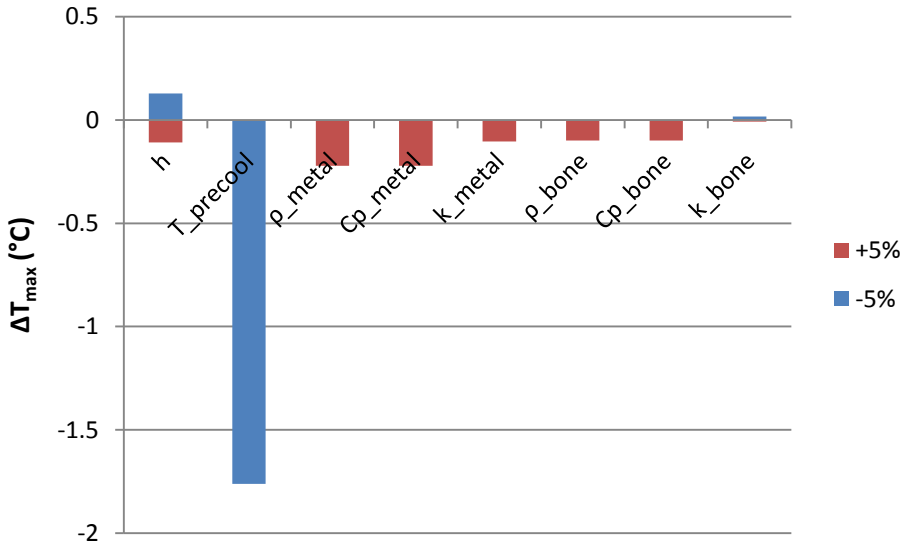

Figure 12. Sensitivity analysis. Parameters were increased and decreased by 5%, while T_{max} was measured.

Figure 13 shows the parameter values that we were able to do a two-sided sensitivity analysis. In both cases, we see that the system was more sensitive to parameter changes that increased T_{max} than those that decreased them. This supports the idea that our computational errors are related to rapid heat generations, as the values for which we weren't able to do the sensitivity analysis were the ones that increased T_{max}.

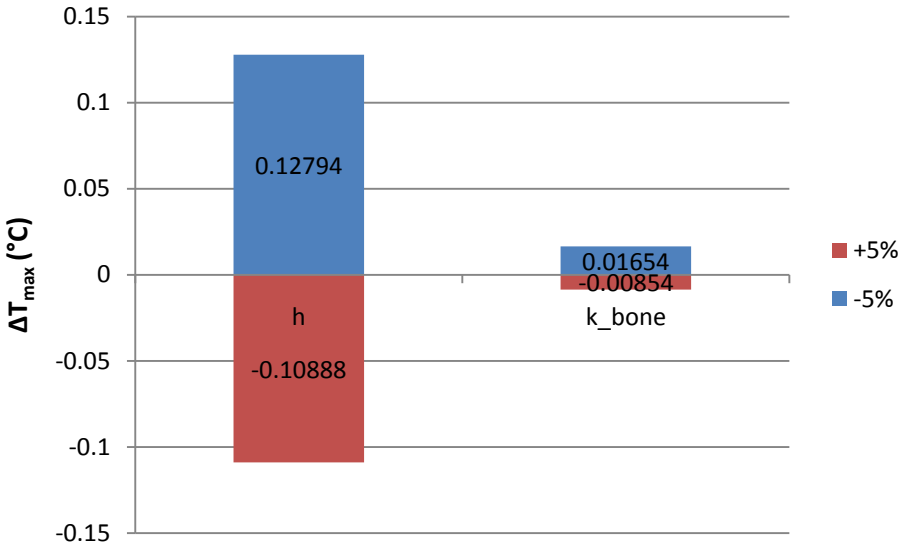

Figure 13. Sensitivity analysis. Parameters were increased and decreased by 5%, while T_{max} was measured.

While the system is rather sensitive to the value of h for the flux boundary condition, it is surprising that it wasn't the most influential parameter. While debugging our model, we found that this value had a large effect on whether or not the system would converge. However, through our analysis it appears that all of our parameters are close to a non-convergent state. For most of the parameters above, we were not able to test smaller values than the defaults to obtain convergence (as indicated by a *). In fact, we were unable to determine the sensitivity for the precooling temperature for the cement because the system would not converge with deviation from the default value.

E. Accuracy Check

In **Figure 14**, one can see that the temperature at our test point in the femur ball stays almost constant at around 33°C up until 700s. At this time, cement polymerization has not happened yet, and simple heat diffusion from the tissue to the cement and the implant takes place in this region. Then, after 700s, polymerization proceeds to its completion within 50s, and temperature rapidly increases to its maximum temperature along with the degree of polymerization. The inside bone-cement interface reaches 53°C , and the outside bone-cement interface reaches slightly less than that, around 46°C. After polymerization is completed and the temperature peak is reached at 750s, the heat generated in the cement is diffused out to the tissue and the temperature of the cement gradually drops to around 33°C at 2000s.

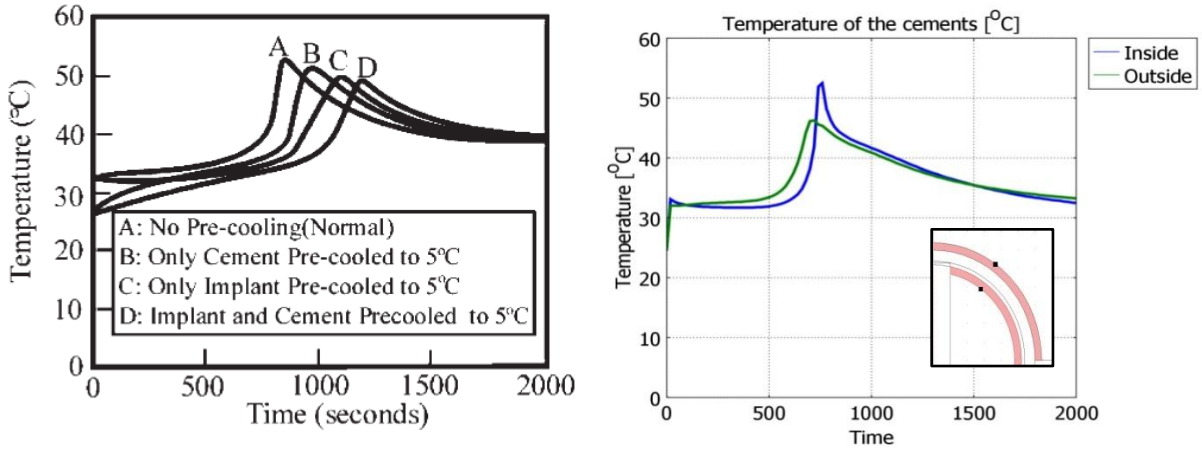

Figure 14. Temperature profiles at the bone-cement interfaces in Li et al. (left) and in our model (right). The coordinates are indicated as ■. (coordinates: inner interface [0.01347, 0.019961] and outer interface [0.017086, 0.027193]) In the model on the right, initial temperature for bone, cap, and ball was 25°C without precooling. Thus, both lines – temperature profile of the inner cement and the outer cement with the same initial condition – on the right figure corresponds to A in the left figure.

In order to check whether the computational model we established is accurate, the results were compared in **Figure 14** with Li et al. The geometry of our and the model in Li et al., 2003 are not exactly the same. Li et al. made a 1D model for thermal necrosis from cement polymerization in total hip replacement. In contrast, our model is a 2D model with a spherical shape, and the convection term is included as a boundary condition. However, both models use the same polymerization kinetic model and the basic heat transfer pattern is similar (from cement to the surrounding tissue on the one side and the replacement on the other). Thus, we expect that obtaining a similar temperature and polymerization profile would qualify our computational design**.**

Despite the geometrical differences, the two models showed great similarity. The onset of polymerization in both models occurs around and before 700s; the temperature profiles match very well. Moreover, they both reach T_{max} around 750s. However, in our model, the temperature of the interface settles around 35°C a long time after the completion of polymerization whereas in Li's et al. (2003) shows that the equilibrium temperature is higher. Possible explanations for the differences are because our model has a larger tissue region for the heat from polymerization to be diffused out and because the air convection from the surface of the bone transfers heat out of the system.

4. Conclusion

A. General Conclusions

1) **Precooling may be an effective means to prevent thermal necrosis.** We simulated some success with that approach by cooling the ball and cap to 277K and leaving the cement at room temperature (298K). Our simulation also shows that although the cement may be cooled to 277K as well, it may not affect the maximum temperatures in any significant way. By extension, it

would seem that precooling could be advantageous in any surgical process that involves polymerization, as heat generation is a potential danger (i.e. thermal necrosis).

2) Cancellous bone may be less prone to thermal necrosis during surgery, which suggests that **HRA may not be as damaging to the elderly** as previously thought. This certainly deserves further consideration, especially as resurfacing advances.

3) **While our computational failure caused by the generation of "hot spots" likely does not reflect realistic physics, the issue deserves further investigation.** Our convergent solutions revealed that the regions that become these problematic "hot spots" in the nonconvergent case reach high values. The computational failure in the nonconvergent case may reflect a potentially very dangerous thermal condition. Additional testing must be done to determine how this phenomenon manifests in real-life situations.

4) **It is important to ensure sufficient time is given for the polymerization to finish in all areas of the prosthetic**. During cement polymerization, heat first diffuses into the cement which triggers its polymerization and ensuing heat generation. The outer cement is triggered first because of the larger surface area adjacent to the tissue, but heat generation terminates quickly because heat from the polymerization diffuses out from the cement to the tissue faster than the inner cement. Although the degree of polymerization reaches from 20% to 90% rapidly, the finishing process (from 90% to 100%) may be quite slow.

5) Our value for the heat transfer coefficient at the convective boundary was decided largely due to the fact that we were able to avoid computational failure, but it's interesting to consider the possibility that **convective cooling could be an effective means to reduce thermal necrosis**. Though there may be some promise here, there are likely downsides with high convection (drying tissues, etc.). Our sensitivity did show that there was some sensitivity to the heat transfer coefficient, but it wasn't nearly as significant as the precooling temperature.

The American Association of Hip and Knee Surgeons discuss a variety of considerations that are needed. As medical technology regarding hip joints is advancing, surgery must be minimally invasive to reduce surgical complications. The lower bound for how invasive a surgery can be is ultimately related to ethical issues for surgeons as their dexterity decides what the minimum possible incision may be. Soft tissues always suffer trauma during and after surgery, and less invasive surgery decreases immediate post-pain, and blood loss (leading to fewer transfusions). It also preserves normal tissue intervals and decrease muscle damage.

While hip resurfacing arthroplasty preserves more bone parts than total hip replacements, it is important for the surgeons to be more knowledgeable of the risk involved due to the thermal conditions of HRA that may damage the "saved bone" inside the ball.

B. Design Recommendations and Realistic Constraints

In terms of economic feasibility, the precooling procedure is promising because it does not involve any significant cost for surgeons to apply the technique and seems to have a significant effect on maximum temperature. There have been issues with slow polymerization in the precooled cement; however, our model confirmed that while precooled cement may

polymerize slowly, complete polymerization is still reached within 1500s. We expect that this prolonged time of 25 minutes is not significantly problematic.

The elderly patients who have cancellous bone actually suffer less from thermal necrosis because of reduced heat transfer through the bone. Currently, total hip replacement technique is preferred instead for the elderly patients for a number of reasons, namely that it tends to be a more robust surgery, as weaker bone is being replaced with a metal prosthetic. However, if the strength of the hip resurfacing arthroplasty is improved to be comparable with that of total hip replacement in the future, hip resurfacing arthroplasty should be considered an alternative to the elderly patients because it is less intrusive and because the thermal necrosis of HRA can be a less serious concern for the elderly.

Appendices

Appendix A: Mathematical statement of the problem

Governing Equation:
Governing equation for heat transfer in the bone and the replaced parts

$$\rho c_p \frac{\delta T}{dt} = k\left(\frac{1}{r}\frac{\delta}{\delta r}\left(r\frac{\delta T}{\delta r}\right) + \frac{\delta^2 T}{\delta z^2}\right) + Q$$

Assumptions:

1) Transient: temperature of the tissues changes in time.
2) No convection: tissue and bone are solid; they do not flow like fluid.
3) Heat diffuses through the tissue.
4) Heat generation is only from the cement mantle.
5) Heat diffusion is symmetric with respect to direction φ.

Relevant Equations:

The applied heat generation term Q (Eq. 1) comes from the polymerization of the cement mantle, and the equation is found from Li, 2003. α is the degree of polymerization. $z_0 = 5.206 \times 10^9 s^{-1}$, $E_a = 67891 \frac{J}{mol}$, m=1.05, n=1.10 (Li, 2003). $Q_{tot} = 125 \frac{J}{g}$ (For PMMA, Maffezzoli, 1996)

$$Q = \begin{cases} \rho Q_{tot} \frac{d\alpha}{dt} & \text{for the cement mantle} \\ 0 & \text{for the bone and implant} \end{cases} \quad \text{.....(Eq. 1)}$$

$$\frac{d\alpha}{dt} = Z_0 e^{-\frac{E_a}{RT}} (1-\alpha)^n \alpha^m$$

Since bone necrosis is our main parameter of interest, we created a thermal damage factor at a point x. $\Omega(x)$ is defined by Moritz and Henrique (1947). Cell necrosis will occur at any temperature greater than 44°C.

$$\Omega(\mathrm{x}) = \mathrm{A}_1 \int_0^{\mathrm{t}} \mathrm{e}^{-\frac{\mathrm{A}_2}{\mathrm{T(x,t)}}} \mathrm{dt}$$

T(x,t) is the temperature history at the investigated point x. $A_1 = 8.013 \times 10^{62} s^{-1}$ and $A_2 = 4.865 \times 10^4 K$ are constants evaluated from experiments. Here, $\Omega > 0.4$ indicates osteocyte necrosis.

When implementing the governing equation above in COMSOL, we used three application modes: transient heat transfer application mode for the main governing equation, transient diffusion applications for both the degree of polymerization and the thermal damage factor.

As shown above, mathematical transformation of the two equations fits well with the transient diffusion equation with no diffusion and no convection. In COMSOL, we set D and u

equal to zero and put the right-hand side of the equations into reaction rate terms. The degree of polymerization was only applied to the cement region, and the thermal necrosis factor only to the bone region. Other regions were set to be inactive in COMSOL.

Initial Conditions:

1) Initial temperature of the bone cement = 25˚C
2) Initial temperature of the other parts (cup, ball, and bone) =37˚C
3) Initial condition for the polymerization equation: α = 1.02×10-4 (Li, 2003)
4) Initial thermal damage factor of the bone = 0

Boundary Conditions:

1) Convection heat transfer (yellow dotted line from **Figure 2**). h = 100W/m^{2}K for air, T_∞=25˚C, and n is the normal direction

$$-k\frac{\partial T}{\partial n} = h(T_\infty - T)$$

2) No heat flux (blue dotted line from **Figure 2**) from both semi-infinite assumption and symmetry.

$$\frac{\partial T}{\partial n} = 0$$

Material Properties:

Table 1. Material properties considered in our simulation. Default values are shown in red, while yellow values signify the different test conditions.

	Implant				Bone		Cement
Parameter	CoCr	Zirconium	Tantalum	Alumina	Normal	Cancellous	PMMA
$\rho\ \left[\frac{kg}{m^3}\right]$	8800	6520	16690	3960	1850	620	1683
$C_p\ \left[\frac{J}{kg \cdot K}\right]$	434	278.0	140	753	[1140-2370] avg = 1755	4926	310
$k\ [\frac{W}{m \cdot K}]$	14.7	22.7	57.5	46.0	[0.16-0.34] avg = 0.25	0.39	0.12

Appendix B: Solution Strategy

Mesh and Mesh Convergence

To analyze the heat diffusion pattern of the hip replacement system, COMSOL Multiphysics was used. COMSOL analyzed the transient heat conduction equation and the transient diffusion equation (the equation for degree of polymerization). Our time step was every 20 seconds for 2000 seconds. Calculations were performed with a 0.01 relative tolerance, and a 0.0010 absolute tolerance. Linear system solver was used and the direct solving method UMFPACK was employed.

Due to the complicated geometry of the system, three-noded triangle mesh was used and meshes were unstructured although we selectively refined the mesh around the cement regions. Heat is generated from those regions, so the greatest temperature change occurs there.

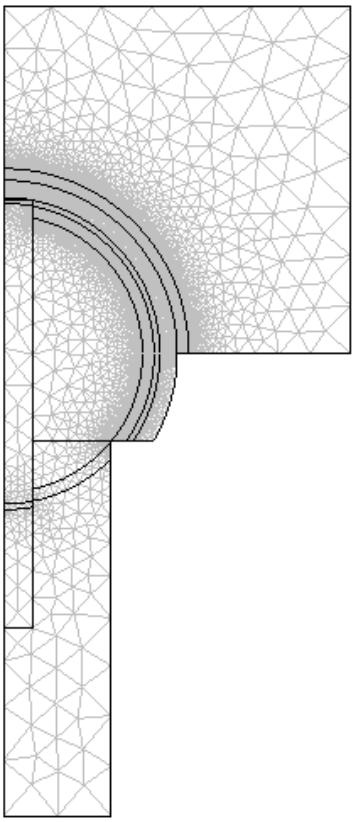

\

Figure 15. Mesh plot of the hip replacement system

Table 2. Mesh Convergence Analysis

Number of mesh	Value of surface integral [m^2K]	Average Temperature of the outside cement (subdomain 8)[K]	Differences [K]
1135	0.030287	310.988766	3.306315669
2164	0.030609	314.2950817	-1.262971513
4949	0.030486	313.0321102	0.359382138
5529	0.030521	313.3914923	0.308041832
8143	0.030551	313.6995341	-0.082144489
16578	0.030543	313.6173897	0.071876428
24600	0.03055	313.6892661	-0.061608366
40099	0.030544	313.6276577	0

The average temperature of the inside cement region was calculated for the mesh convergence. The temperature values over the region was integrated, then divided by the volume of the sub-domain. The volume of the sub-domain was determined by integrating the sub-domain region 8 with value 1 instead of the temperature values.

The number of elements was tested in the range of 1135 - 40099. With element numbers greater than 40099, the computer does not have enough memory to support the solution process. From **Figure 16**, it is possible to recognize the region where the average temperature stops oscillating and starts to converge. From 20000 elements onward, the average temperature starts to converge and does not oscillate.

However, with the number of elements from 1135 to about 5529, the average temperature values fluctuate largely. The magnitude of the fluctuation was calculated by getting the difference of average temperature between each node.

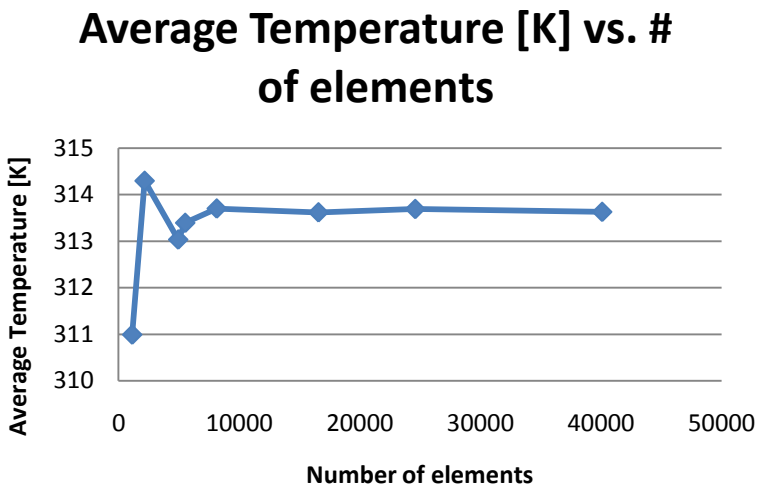

Figure 16. Mesh convergence analysis. Mesh Convergence: Average Temperature (in Kelvin) vs. number of elements

The average temperature converges to a difference of only about 0.06-0.08K between 16578 and 40099 elements. As expected, the average temperature value fluctuated most greatly with lower number of elements. The average temperature jumped by 3.3 K (from 310.989K to 314.295K) when the number of meshes increased from 1135 to 2164. The difference gradually decreases to 0.06 K as described above.

Thus, the default solution was obtained by setting the number of elements 34496, which is inside the range where the convergence of values happens.

Appendix C: Additional Visuals

The temperature contour plot animation is included in electronic submission. The video is snap shots of temperature contour plot representing our general solution with respect to varying time. The temperature contour plot animation displays the heat generation in cement and the heat

propagation from the cement into the bones and how the convective cooling along the boundaries have effect on temperature profile with change of time.

Surface plots for volumetric heat generation at 760 seconds (**Figure 17**) shows a similar pattern with temperature surface plot, showing the rippling effect of heat generation from the cement.

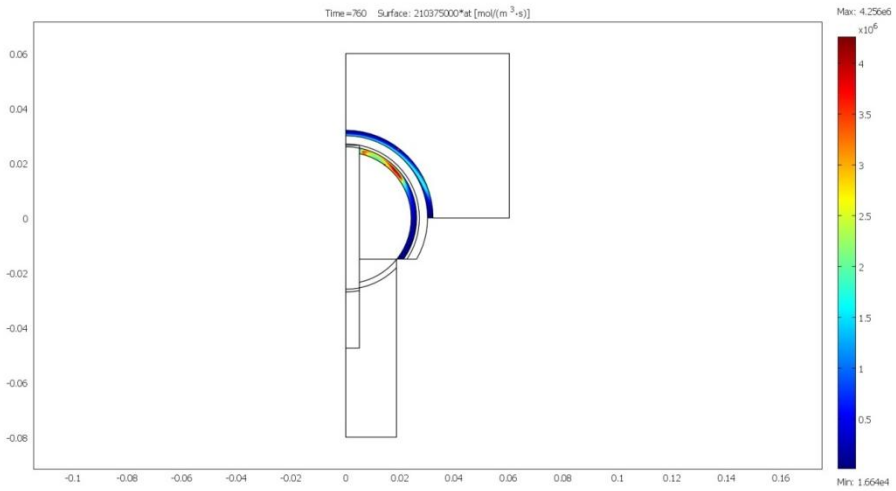

Figure 17 Volumetric heat generation Q (in W/m^3) at 760 seconds. In order to model the source term, we implemented the degree of polymerization using a COMSOL diffusion physics system.

Appendix D: Sources and References

Table 3. Sources of Material Properties (**continued** next page)

Material Properties	Value	Source
Alumina		
ρ [kg/m^3]	3960	http://www.matweb.com/search/DataSheet.aspx?MatGUID=c8c56ad547ae4cfabad15977bfb537f1
C_p [J/kg-K]	753	http://www.matweb.com/search/DataSheet.aspx?MatGUID=c8c56ad547ae4cfabad15977bfb537f1
k [W/m-K]	46.0	http://www.matweb.com/search/DataSheet.aspx?MatGUID=c8c56ad547ae4cfabad15977bfb537f1
CoCr Alloy		
ρ [kg/m^3]	8800	http://www.matweb.com/search/datasheet.aspx?matguid=84df9b15899942ee9a8e66ba93e6ae29&ckck=1
C_p [J/kg-K]	434	http://iadr.confex.com/iadr/pef08/techprogram/abstract_110905.htm
k [W/m-K]	14.7	http://www.matweb.com/search/datasheet.aspx?matguid=84df9b15899942ee9a8e66ba93e6ae29&ckck=1
Zirconium		
ρ [kg/ m^3]	6520	David R. Lide (ed), CRC Handbook of Chemistry and Physics, 84th Edition. CRC Press. Boca Raton, Florida, 2003; Section 4, Properties of the Elements and Inorganic Compounds; Physical Constants of Inorganic Compounds
C_p [J/kg-K]	278.0	David R. Lide (ed), CRC Handbook of Chemistry and Physics, 84th Edition. CRC Press. Boca Raton, Florida, 2003; Section 4, Properties of the Elements and Inorganic Compounds; Heat Capacity of the Elements at 25°C
k [W/m-K]	22.7	David R. Lide (ed), CRC Handbook of Chemistry and Physics, 84th Edition. CRC Press. Boca Raton, Florida, 2003; Section 12, Properties of Solids; Thermal and Physical Properties of Pure Metals / Thermal Conductivity of Crystalline Dielectrics / Thermal Conductivity of Metals and Semiconductors as a Function of Temperature
Tantalum		
ρ [kg/ m^3]	16690	David R. Lide (ed), CRC Handbook of Chemistry and Physics, 84th Edition. CRC Press. Boca Raton, Florida, 2003; Section 4, Properties of the Elements and Inorganic Compounds; Physical Constants of Inorganic Compounds
C_p [J/kg-K]	140	David R. Lide (ed), CRC Handbook of Chemistry and Physics, 84th Edition. CRC Press. Boca Raton, Florida, 2003; Section 4, Properties of the Elements and Inorganic Compounds; Heat Capacity of the Elements at 25°C
k [W/m-K]	57.5	David R. Lide (ed), CRC Handbook of Chemistry and Physics, 84th Edition. CRC Press. Boca Raton, Florida, 2003; Section 12, Properties of Solids; Thermal and Physical Properties of Pure Metals / Thermal Conductivity of Crystalline Dielectrics

Table3 continued. Sources of Material Properties

NormalBone		
ρ [kg/ m^3]	1850	Cameron, J.R.,Skofronick, J.G., and Grant, R.M. Physics of the Body. Second Edition. Madison, WI: Medical Physics Publishing, 1999: 96.
C_p [J/kg-K]	1140-2370	Suleyman, B., Modest, M.F.,Tarr, R. Measurements of thermal properties for human femora.
k [W/m-K]	0.16-0.34	Suleyman, B., Modest, M.F.,Tarr, R. Measurements of thermal properties for human femora.
CancellousBone		
ρ [kg/ m^3]	620	An Y.H.,Draugh, R.A. Mechanical Testing of Bone and the Bone-implant Interface. First Edition. CRC Press, 1999.
C_p [J/kg-K]	4926	Clattenburg, R. and Cohen, J. Thermal Properties of Cancellous Bone. Journal of Biomedical Materials Research 1975 (9): 169-182.
k [W/m-K]	0.39	Clattenburg, R. and Cohen, J. Thermal Properties of Cancellous Bone. Journal of Biomedical Materials Research 1975 (9): 169-182.
PMMA (cement)		
ρ [kg/ m^3]	1683	Hung, et. al. Further Analytical Study of Hybrid Rocket Combustion. NASI-10210, 1972.
C_p [J/kg-K]	310	Hung, et. al. Further Analytical Study of Hybrid Rocket Combustion. NASI-10210, 1972.
k [W/m-K]	0.12	Hung, et. al. Further Analytical Study of Hybrid Rocket Combustion. NASI-10210, 1972.

Bibliography

Chandler, M., Kowalski, RSZ., Watkins, N.D., Briscoe, A., New, AMR. Cementing Techniques in Hip Resurfacing. Proceedings of the Institution of Mechanical Engineers.Vol 220 (2005): Part H- Journal of Engineering in Medicine.

Greenspan, A., Norman, A. Gross Hemeturia: A Complication of Intrapelvic Cement Intrusion in Total Hip Replacement. American Journal of Roentgeneology.Vol 130(1978): 327-329.

Iesaka, K., et al. Effects of the Initial Temperature of Acrylic Bone Cement Liquid Monomer on the Properties of the Stem-Cement Interface and Cement Polymerization. Journal of Biomedical Materials Research Part B: Applied Biomaterials. 68B(2004): 186-190

Li, C., Schmid, S., Mason, J. Effects of pre-cooling and pre-heating procedures on cement polymerization and thermal osteonecrosis in cemented hip replacements. Medical Engineering and Physics. Vol 25 (2003): 559–564.

Maffezzoli, A. Polymerization Kinetics of Acrylic Bone Cements by Differential Scanning Calorimetry.Journal of Thermal Analysis.Vol 47(1996): 35-49.

"Minimally Invasive and Small Incision Joint Replacement Surgery." American Association of Hip and Knee Surgeons. Rosemont, Illinois: January 2008.
Okrajni, J., et al. Computer Modeling of the Heat Flow in Surgical Cement During Endoprosthesoplasty. Journal of Achievements in Materials and Manufacturing Engineering. 20.1-2(2007): 311-314.

Sanchez, M., et al. Computer Simulation of Realistic Three-Dimensional Cemented Hip Arthroplasty: Thermal Osteonecrosis Analysis. Journal of Thermophysics and Heat Transfer. 22.4 (2008): 741-748.

Throne, James. Technology of Thermoforming. Cincinnati, Verlag, 1996. 124. From < http://books.google.com/books?id=n8gRZho52IYC&pg=PA124>

Videbaek, P.A.,Sommer, S. Urological Complications after Total Hip Replacement. Archives of Orthopaedic and Traumatic Surgery.Vol 104 (1985): 132-134.